Control of Thermal Emission by Selective Heating of Periodic Structures

S. E. Han and D. J. Norris*

Department of Chemical Engineering and Materials Science, University of Minnesota, Minneapolis, Minnesota 55455, USA
(Received 23 September 2009; published 25 January 2010)

We predict that thermal emission can be controlled by selective heating of periodic structures. Previous studies on thermal emission modification via photonic crystals have been limited to uniform temperature. We consider frequency-dependent nonuniform absorption in a periodic structure and show that thermal emission peaks can be associated with specific locations in the structure. Consequently, local periodic heating allows control over which peaks appear in the thermal emission spectrum, as we demonstrate with calculations on two-component metallodielectric structures.

When a material is structured on a micrometer length scale, its thermal emission spectrum can be modified. This can occur due to excitation of optical modes on patterned surfaces [1–3] or due to optical diffraction in three-dimensionally periodic solids known as photonic crystals [4–6]. By utilizing these effects, heated structures can exhibit thermal emission over a relatively narrow spectral range, instead of a broad blackbody-like peak. This may lead to efficient light sources, new thermophotovoltaic devices [7,8], and unexpected physical phenomena. However, so far, investigations have been limited to structures that are homogeneously heated. In this case, all electromagnetic modes that conserve energy and can couple to propagating modes in the far field will emit. If instead, heat is applied inhomogeneously, additional control over the emission might be possible. Consider monochromatic light coupled from the far field into a photonic crystal with a lattice parameter comparable to the optical wavelength. Diffraction will concentrate this electromagnetic wave at specific locations within the unit cell, analogous to spatial variations in the electronic wave functions of atomic crystals [9]. If this photonic crystal were heated periodically with the same pattern, a specific frequency might be selected for thermal emission. Thus, depending on where the heat is applied within the unit cell, spectral control over the thermal emission might be obtained.

In this Letter, we examine this simple and surprisingly unexplored possibility. Because Kirchhoff's law, which is the typical starting point for modeling thermal emission, is not applicable when local temperature variations exist, we use instead the reciprocity theorem of electrodynamics. It roughly states that a fluctuating current and the electric field that it creates at a distant location can be interchanged without affecting their relationship [10,11]. Thus, if an external field of a specific frequency is concentrated within the structure, oscillating dipoles placed at the same locations will lead to strong emission at this frequency. Below, we combine the reciprocity theorem with the fluctuation-dissipation theorem and examine structures in which the absorptivity periodically varies in space. We show that

thermal emission can be controlled depending on how the heat is applied within the unit cell. For example, numerical calculations for a two-component structure show that one can choose between two emission frequencies depending on which component is heated. Thus, we confirm that nonuniform heating can provide new control over thermal emission.

To begin, we derive an expression for the emission intensity $\mathcal{P}$ emanating from a thin photonic film consisting of periodically placed components. The film lies in the xy plane with a finite thickness in z. We first make an important assumption, addressed further below, that the fluctuation-dissipation theorem is valid locally. Maxwell's equations can then be solved for thermal emission propagating away from the structure at an angle θ from the z axis. The emission rate per unit solid angle per unit frequency per unit area is

$$\mathcal{P}_{+\boldsymbol{\kappa}}^{\alpha+} = \frac{\int_{S_{uc}} d\boldsymbol{r}_{\parallel} \int dz Q_{-\boldsymbol{\kappa}}^{\alpha-}(\boldsymbol{r}_{\parallel}, z) \mathcal{P}_{BB}^{\alpha+}(\boldsymbol{r}_{\parallel}, z)}{S_{uc} \cos\theta}. \quad (1)$$

A detailed derivation of Eq. (1) can be found in Ref. [12,13]. Here, α designates the polarization of the light (TE or TM) while $+$ and $-$ indicate whether the light is propagating away from or toward the film, respectively. S_{uc} is the area of a two-dimensional unit cell in the xy plane, and $\boldsymbol{\kappa}$ and $\boldsymbol{r}_{\parallel}$ are the wave vector and the position vector parallel to this plane. $Q_{-\boldsymbol{\kappa}}^{\alpha-}$ is the local absorption rate per unit volume for a film irradiated with polarized light of unit intensity and is given by

$$Q_{-\boldsymbol{\kappa}}^{\alpha-}(\boldsymbol{r}_{\parallel}, z) = \frac{\omega}{c} \varepsilon_I(\boldsymbol{r}_{\parallel}, z) \frac{|\boldsymbol{E}_{-\boldsymbol{k}_{\parallel}}^{\alpha-}(\boldsymbol{r}_{\parallel}, z)|^2}{|\tilde{\boldsymbol{E}}^{\alpha-}|^2}, \quad (2)$$

where c and ω are the speed and angular frequency of the light, ε_I is the imaginary dielectric function, $\boldsymbol{k}_{\parallel}$ is the component of $\boldsymbol{\kappa}$ in the first Brillouin zone, $\boldsymbol{E}_{-\boldsymbol{k}_{\parallel}}^{\alpha-}$ is the electric field inside the film with $-\boldsymbol{k}_{\parallel}$ when irradiated by light of polarization α and parallel wave vector $-\boldsymbol{\kappa}$, and $\tilde{\boldsymbol{E}}^{\alpha-}$ is the Fourier component of the electric field for an incident plane wave with parallel wave vector $-\boldsymbol{\kappa}$. $\mathcal{P}_{BB}^{\alpha+}$ is

the blackbody radiation intensity given by

$$\mathcal{P}_{BB}^{\alpha+}(\boldsymbol{r}_{\parallel}, z) = \frac{\hbar\omega^3}{8\pi^3 c^2} \frac{1}{e^{\hbar\omega/k_B T} - 1}, \qquad (3)$$

where $\hbar$, k_B, and T are Planck's constant, Boltzmann's constant, and temperature. Although not explicitly stated, $\mathcal{P}$, Q, ε_I, and $\boldsymbol{E}$ depend on ω, and due to nonuniform T, $\mathcal{P}_{BB}^{\alpha+}$ depends on position.

Note that Eq. (1) states that the emission $\mathcal{P}$, which is caused by current fluctuations, is related to the absorption rate Q, as required by the fluctuation-dissipation theorem. Also, $\mathcal{P}_{+\boldsymbol{\kappa}}^{\alpha+}$ is related to the absorption rate for light propagating in the opposite direction, i.e., $Q_{-\boldsymbol{\kappa}}^{\alpha-}$, as required by the reciprocity theorem.

Next, we assume that the structure consists of two material components labeled 1 and 2 with temperatures T_1 and T_2. In this case, Eq. (1) can be reduced to

$$\mathcal{P}^{\alpha+} = A_1^{\alpha-} \mathcal{P}_{BB}^{\alpha+}(T_1) + A_2^{\alpha-} \mathcal{P}_{BB}^{\alpha+}(T_2), \qquad (4)$$

where $A_i^{\alpha-}$ is given by

$$A_i^{\alpha-} = \frac{\int_{S_i} d\boldsymbol{r}_{\parallel} \int dz Q_{-\boldsymbol{\kappa}}^{\alpha-}(\boldsymbol{r}_{\parallel}, z)}{S_{uc} \cos\theta}, \qquad (5)$$

with S_i as the area of component i in the xy unit cell. For simplicity, we do not include the dependence of $A_i^{\alpha-}$ on $\boldsymbol{k}_{\parallel}$ in our notation. $A_i^{\alpha-}$ is a useful parameter for describing photonic structures. Because the overall absorptivity $A^{\alpha-}$ for α polarization is the sum

$$A^{\alpha-} = A_1^{\alpha-} + A_2^{\alpha-}, \qquad (6)$$

$A_i^{\alpha-}$ represents the local contribution of component i. Thus, we refer to it as the local absorptivity. Here, we make a connection to an analogous parameter, the local density of photonic states (LDOS). LDOS helps quantify the contribution of an individual optical dipole at a specific location in a photonic crystal to the spontaneous emission from a distribution of dipoles [14,15]. Similarly, Eq. (4) shows that the local absorptivity can describe specific spatial contributions to the thermal emission intensity. Consequently, once all $A_i^{\alpha-}$ are known, the thermal emission can be obtained for various temperature configurations. Because of this relationship to emission, $A_i^{\alpha-}$ could alternatively be called the local emissivity.

To be useful for spectral control of thermal emission, the two components in Eq. (4) must have local absorptivities that peak at different energies. We demonstrate this possibility with calculations for a specific structure [16]. Two layers of parallel tungsten and silicon rods lie in the plane of the film (the xy plane). The rods are arranged as in the cross section in Fig. 1. This structure repeats in the x direction; the rods are uniform in y. (See also Fig. S1 in [12].) We used experimental dielectric functions [17] and assumed a donor concentration of 3×10^{19} cm^{-3} for Si, so it has an absorption comparable to W near 0.45 eV. Figure 1(a) shows the calculated absorptivity when the film is illuminated along z by TE polarized light (the
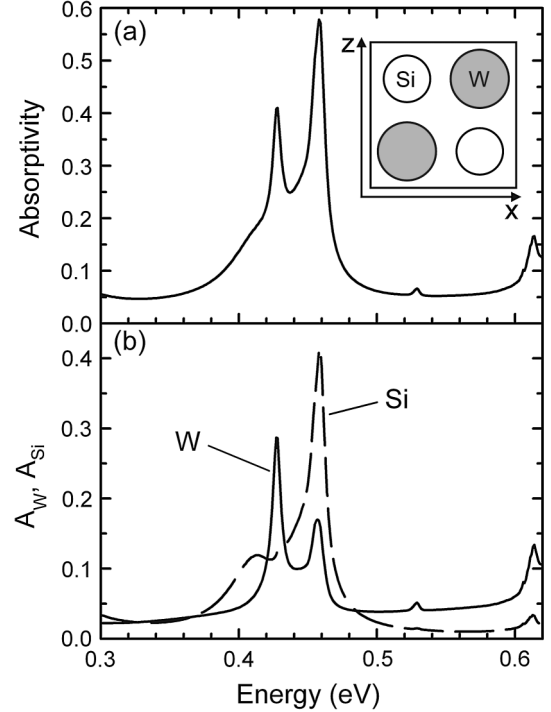

FIG. 1.   Calculated (a) absorptivity and (b) local absorptivities, A_W and A_{Si}, for a film with the cross section in the inset. This structure repeats in the x direction and is uniform in y. The W and Si rods are 800 and 640 nm in diameter, respectively. The center-to-center distance of neighboring rods is 1 μm. The absorptivity is averaged for TE polarized light incident over a cone $\pm 5°$ from the z axis.

magnetic field along the rods). This calculation also averages the absorptivity over $\pm 5°$ from the z axis to approximate experiments. Two pronounced peaks at 0.428 and 0.458 eV are found. The local absorptivities in Fig. 1(b) show that each peak can be attributed primarily either to the W or the Si rods. This occurs because the structure has two resonances which concentrate the light differently in the two rods, as seen in Fig. S2 in [12].

Thus, Eq. (4) suggests that the peak at 0.428 eV will be strong if the W rods are heated and the 0.458 eV peak will dominate if Si is heated. However, we must determine the temperature to apply. Note that the goal is different than with uniform heating, where the temperature is chosen simply to overlap the blackbody spectrum with the absorption to maximize the emission [4]. Here, we want to control the emission frequency. We consider two cases and apply Eq. (4). When W is "hot" and Si is "cold," we label the result $\mathcal{P}_{W\,hot}^{\alpha+}$. The opposite case is $\mathcal{P}_{Si\,hot}^{\alpha+}$. Taking the ratio, we obtain

$$\frac{\mathcal{P}_{W\,hot}^{\alpha+}}{\mathcal{P}_{Si\,hot}^{\alpha+}} = \frac{A_W^{\alpha-} + A_{Si}^{\alpha-}\rho(T_c, T_h)}{A_W^{\alpha-}\rho(T_c, T_h) + A_{Si}^{\alpha-}}, \qquad (7)$$

where T_h and T_c are the temperatures of the hot and cold rods, respectively, and

$$\rho(T_c, T_h) = \frac{\mathcal{P}_{BB}^{\alpha+}(T_c)}{\mathcal{P}_{BB}^{\alpha+}(T_h)} < 1. \qquad (8)$$

From Eq. (8), we see that $\rho(T_c, T_h)$ should be minimized to maximize the intensity contrast for the two peaks. In the ideal case, $\rho(T_c, T_h)$ vanishes and the ratio becomes $A_W^{\alpha-}/A_{Si}^{\alpha-}$. Figure 2 shows $\rho(T_c, T_h)$ as a function of T_c when $T_h - T_c$ is 300 K. Several specific photon energies are plotted. For example, when T_c is 500 K, $\rho(T_c, T_c + 300)$ is about 0.02 at 0.428 and 0.458 eV. Thus, the peak contrast should be nearly ideal at these temperatures. Moreover, they are well below the melting points of the two components (3687 K for W and 1687 K for Si).

The emission intensities obtained from Eq. (4) for $T_c = 500$ K and $T_h = 800$ K are displayed in Fig. 3. As predicted, the two peaks can be controlled depending on which rods are hot. Moreover, the intensity contrast is pronounced at these temperatures. For comparison, we also plot the emission spectra when both rods are 500 K or both 800 K. The results with $T_c = 500$ K and $T_h = 800$ K are bounded by the uniform cases at all photon energies.

Of course, if the goal is to control the energy of a thermal emission peak, approaches other than selective heating are possible. For example, the rod spacing in a uniformly heated structure could simply be modified. In our case, the Si rods could be removed and the emission energy tuned by changing the separation between the W rods. However, we find that the presence of the Si rods actually induces more emission from the W. To show this, we calculated the emission spectrum for our film without the Si rods. Since vacuum now replaces the Si, the optical path length between the W rods decreases. Consequently, the emission peak associated with W appears at higher energy. To compare with the result for the W-Si film, we increased the distance between the W rods by 28% to return the W peak to its original energy (0.428 eV). The resulting emis-
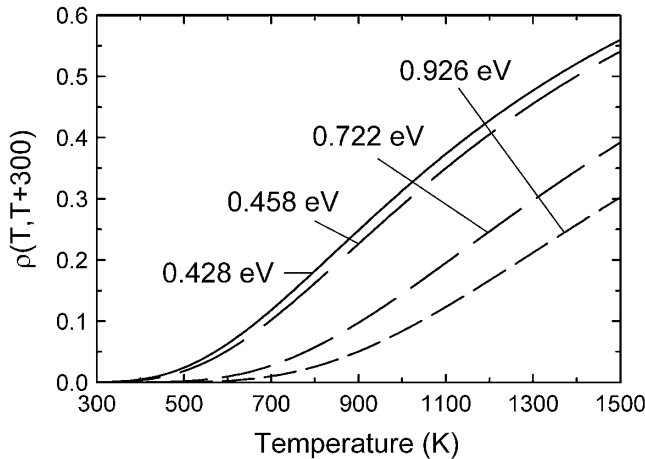
sion spectrum at 800 K is shown as the black line in Fig. 3. The peak is clearly weaker than when W rods are heated to 800 K in the presence of cooler Si rods. This occurs because the Si rods modify the local absorptivity of the W. Thus, selective heating not only provides the ability to control the emission energy with temperature, but the presence of the dielectric rods can also boost the emission. More generally, it allows greater flexibility in the design of emission sources.

If we use different materials, emission control can also be shifted to higher energies. For example, a film similar to above, but with copper and germanium rods, can exhibit emission peaks near the optical wavelength of 1.5 μm (0.83 eV). The rod spacing in the film is adjusted as shown in the cross sectional view in Fig. 4. Figure 4 also plots the calculated intensities for light emitted from the film in the z direction. The temperatures of the rods are the same as in Fig. 3, which are below the melting points of Cu (1358 K) and Ge (1211 K). Two strong peaks appear at 0.722 and 0.926 eV with only broad background emission below 0.6 eV. For this film, the association of each peak with either the metal or the dielectric rods is even stronger than above. Thus, even better control can be obtained. When the Cu rods are hotter than the Ge, the contrast in the two peak intensities is 16.1. In the opposite case, the contrast is 44.1.

The improved contrast in the Cu-Ge film occurs because $\rho(T_c, T_h)$ is smaller at higher energies. At $T = 500$ K, $\rho(T, T + 300)$ is less than 0.002 near 0.83 eV. As seen in Eq. (8), the intensity contrast should increase with decreasing $\rho(T_c, T_h)$. In addition, ε_I for Ge changes significantly between the two emission energies. It varies from 0.004 at 0.722 eV to 0.63 at 0.926 eV. This affects the local absorptivity and, consequently, the emission from the Ge rods is small at 0.722 eV and significant at 0.926 eV, leading to increased contrast.

FIG. 2.   The ratio, $\rho(T, T + 300)$, of the blackbody emission spectra at temperatures T and $T + 300$ versus temperature for several photon energies.
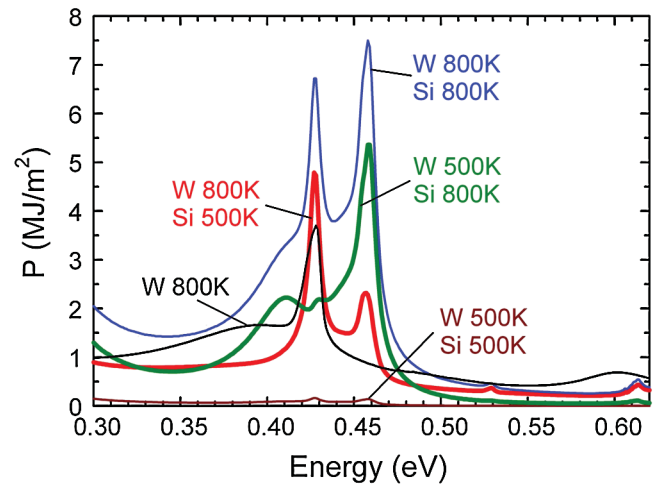

FIG. 3 (color).   Calculated thermal emission intensities for TE polarized light for the W-Si film in Fig. 1. Several temperature combinations are plotted. The emission is averaged over ±5° from the z axis. The black curve is the emission without Si rods; the W rod separation is increased by 28%.
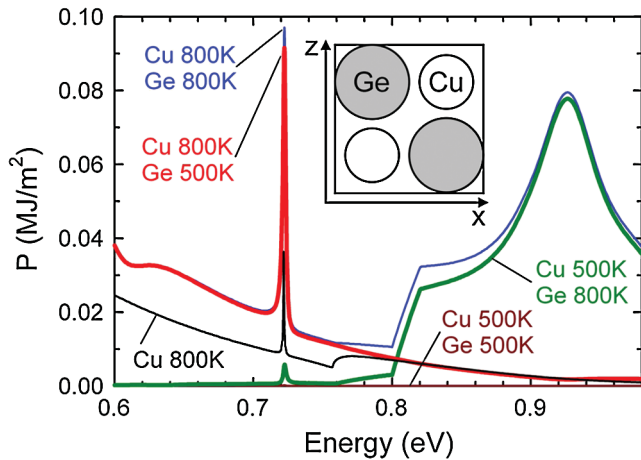
FIG. 4 (color). Thermal emission intensities, calculated as in Fig. 3, for a film of Cu and Ge rods with the cross section shown. This structure repeats in the x direction and is uniform in y. The Cu and Ge rods are 273 and 375 nm in diameter, respectively. The center-to-center distance of neighboring rods is 375 nm. The black curve is the emission without Ge rods; the Cu rod separation is increased by 118%. The kinks at 0.8 and 0.821 eV are due to changes in the Ge dielectric function; the kink at 0.757 eV is due to a Wood's anomaly.

As above, we also considered the film with the dielectric rods removed, in this case Ge. For this calculation, we increased the spacing of the Cu rods by 118% to maintain the energy of the emission peak at 0.722 eV. As seen in Fig. 4, the emission intensity at 800 K for this peak is lower than for the Cu-Ge film. Indeed, the decrease is even more pronounced than for the W-Si film (Fig. 3). Because Ge has a larger dielectric constant than Si ($\sim$17 vs $\sim$11) and occupies more volume in our film, the presence of the Ge rods has a larger influence.

However, two important issues remain: (i) whether such temperature differences can be achieved on a micrometer length scale and (ii) whether our assumption that the fluctuation-dissipation theorem is valid locally is reasonable. In [12], we show that for our structures, thermal conduction along the rods, rather than radiation between them, dominates heat transport. This indicates that if opposite ends of the different rods could be connected to heat reservoirs of different temperatures, the required temperature difference could be obtained. For example, an array of long rods could be fabricated that span a gap between two solid films. The W rods could be connected directly to the top film, but separated thermally from the bottom film by a section of insulating material. The Si rods could be connected oppositely. Thus, by setting the temperatures of the two films, a temperature difference could be achieved. Because thermal transport along the rods dominates, this also implies that local thermal equilibrium should be very nearly satisfied within each rod. In this case, applying the fluctuation-dissipation theorem locally is a reasonable ap-

proximation. More generally, its validity will depend on the specifics of the system and the heating mechanism. If nonequilibrium processes become significant, corrections to the fluctuation-dissipation theorem would be required, and our approach would not be justified.

In conclusion, we predict that thermal emission can be controlled by selective heating of periodic structures. We used the reciprocity theorem which implies that strongly absorbing parts will also strongly emit. In general, selective heating may find applications in active control of thermal light sources. The reverse process, selective absorption, could also lead to local temperature gradients. Thus, further study is required to clarify the full potential and implications of this effect.

*dnorris@umn.edu
[1] P. J. Hesketh, J. N. Zemel, and B. Gebhart, Nature (London) **324**, 549 (1986).
[2] A. Heinzel, V. Boerner, A. Gombert, B. Blasi, W. Wittwer, and J. Luther, J. Mod. Opt. **47**, 2399 (2000).
[3] J. J. Greffet, R. Carminati, K. Joulain, J. P. Mulet, S. Mainguy, and Y. Chen, Nature (London) **416**, 61 (2002).
[4] C. M. Cornelius and J. P. Dowling, Phys. Rev. A **59**, 4736 (1999).
[5] J. G. Fleming, S.-Y. Lin, I. El-Kady, R. Biswas, and K. M. Ho, Nature (London) **417**, 52 (2002).
[6] S. E. Han, A. Stein, and D. J. Norris, Phys. Rev. Lett. **99**, 053906 (2007).
[7] S.-Y. Lin, J. Moreno, and J. G. Fleming, Appl. Phys. Lett. **83**, 380 (2003).
[8] P. Nagpal, S. E. Han, A. Stein, and D. J. Norris, Nano Lett. **8**, 3238 (2008).
[9] J. D. Joannopoulos, R. D. Meade, and J. N. Winn, *Photonic Crystals* (Princeton Univ. Press, New York, 1995).
[10] L. D. Landau and E. M. Lifshitz, *Electrodynamics of Continuous Media* (Pergamon, Oxford, 1984).
[11] S. M. Rytov, Y. A. Kravtsov, and V. I. Tatarskii, *Principles of Statistical Radiophysics*, Elements of Random Fields Vol. 3 (Springer-Verlag, Berlin, 1989).
[12] See supplementary material at http://link.aps.org/supplemental/10.1103/PhysRevLett.104.043901.
[13] S. E. Han, Phys. Rev. B **80**, 155108 (2009).
[14] R. Sprik, B. A. van Tiggelen, and A. Lagendijk, Europhys. Lett. **35**, 265 (1996).
[15] P. Lodahl, A. F. van Driel, I. S. Nikolaev, A. Irman, K. Overgaag, D. Vanmaekelbergh, and W. L. Vos, Nature (London) **430**, 654 (2004).
[16] Throughout, we used the transfer matrix formalism and the unit cell was discretized by a 96×96 mesh.
[17] D. W. Lynch and W. R. Hunter, in *Handbook of Optical Constants of Solids*, edited by E. D. Palik (Academic Press, Orlando, 1985).